



Research paper

Lipid nanoparticles as vehicles for topical psoralen delivery: Solid lipid nanoparticles (SLN) versus nanostructured lipid carriers (NLC)

Jia-You Fang^{a,*}, Chia-Lang Fang^b, Chi-Hsien Liu^c, Yu-Han Su^a^aPharmaceutics Laboratory, Chang Gung University, Taoyuan, Taiwan^bDepartment of Pathology, Taipei Medical University, Taipei, Taiwan^cGraduate Institute of Biochemical and Biomedical Engineering, Chang Gung University, Taoyuan, Taiwan

ARTICLE INFO

Article history:

Received 18 February 2008

Accepted in revised form 9 May 2008

Available online 5 June 2008

Keywords:

Solid lipid nanoparticles

Nanostructured lipid carriers

Psoralen

Topical delivery

Psoriasis

ABSTRACT

Solid lipid nanoparticles (SLN) were developed by using Precirol ATO 5 as the solid core of the particles for topical psoralen delivery. Nanostructured lipid carriers (NLC) consisting of Precirol and squalene, a liquid lipid, were also prepared for comparison. SLN and NLC showed respective mean particle sizes of ~300 and 200 nm, respectively. Viscosity, polarity, and differential scanning calorimetry (DSC) studies were performed to characterize the physicochemical properties of the SLN and NLC. The viscosity of all nanoparticulate systems exhibited Newtonian behavior except the NLC with Tween 80 and soybean phospholipids as the emulsifiers (NLC-Tw). According to the DSC thermograms, the melting peak of Precirol shifted from 58 to 55 °C after incorporating squalene into the solid lipid cores (of NLC), which suggests defects in the crystalline lattice of the lipid cores and smaller particle sizes. Three psoralen derivatives for psoriasis treatments were loaded in SLN and NLC to examine their ability to permeate skin. The permeability of psoralens increased in the order of 8-methoxypsoralen (8-MOP) > 5-methoxypsoralen (5-MOP) > 4,5,8-trimethylpsoralen (TMP). Enhanced permeation and controlled release of psoralen delivery were both achieved using the NLC. The *in vitro* permeation results showed that NLC-Tw increased the 8-MOP flux 2.8 times over that of a conventional emulsion. Hyperproliferative or psoriasis-like skin produced by repeated strippings in the dorsal skin of nude mouse was also used as a permeation barrier. The results showed that the entrapment of 8-MOP in nanoparticulate systems could minimize the permeation differentiation between normal and hyperproliferative skin compared to the free drug in an aqueous control.

© 2008 Elsevier B.V. All rights reserved.

1. Introduction

Solid lipid nanoparticles (SLN) are the new generation of nanoparticulate active-substance vehicles and are attracting major attention as novel colloidal drug carriers for topical use. Compared with other vehicles such as creams, tinctures, and emulsions, SLN combine such advantages as controlled release, negligible skin irritation, and protection of active compounds [1]. Moreover, the small particle sizes of SLN ensure that the nanoparticles are in close contact with the stratum corneum (SC), thus promoting the amount of the encapsulated agent which penetrates into the skin [2]. Nanostructured lipid carriers (NLC) are a new generation of SLN. SLN consist of pure solid lipids, while NLC are made of a solid matrix entrapping variable liquid lipid nanocompartments [3]. Problems associated with SLN such as limited drug loading

capacity, adjustment of drug release, and drug expulsion during storage are avoided by this new generation of carriers.

Psoriasis is one of the most common human skin diseases and is considered to have key genetic underpinnings. It is characterized by excessive growth and aberrant differentiation of keratinocytes [4]. Psoriasis almost always recurs after appropriate therapy. Photochemotherapy with psoralens and long-wavelength ultraviolet (UV) radiation (psoralen and UVA light therapy, PUVA) is a therapy which shows a good clearance rate in psoriasis patients [5]. The psoralens mainly used in PUVA are 8-methoxypsoralen (8-MOP), 5-methoxypsoralen (5-MOP), and 4,5,8-trimethylpsoralen (TMP). Psoralens have strong absorption bands in the range of 200–350 nm. The planar aromatic structure and hydrophobic nature facilitate their intercalation with DNA bases. The absorption of a photon by a psoralen molecule in the ground state can promote an electron to the excited singlet state [6]. Upon photoactivation of the intercalated psoralen molecule, the adducts with thymine and cytosine can be formed. Psoriasis would be relieved by the DNA photoadduct formation that would cause slower cell replication [7]. Studies have shown that the applica-

* Corresponding author. Pharmaceutics Laboratory, Graduate Institute of Natural Products, Chang Gung University, 259 Wen-Hwa 1st Road, Kweishan, Taoyuan, Taiwan. Tel.: +886 3 2118800x5521; fax: +886-3-2118236.

E-mail address: fajy@mail.cgu.edu.tw (J.-Y. Fang).

tion of an emulsion cream and a microemulsion of 8-MOP provides good location of the drug [8,9]. However, there is still a need to develop novel systems formulated with non-irritating components that can be applied to efficiently treat psoriasis. Due to the lipophilic nature of their matrices, SLN and NLC are considered particularly useful for the administration of lipophilic psoralens.

The aim of this study was to develop SLN and NLC, nanoparticulate lipid-based drug carriers, with increased skin permeation and controlled release properties for psoralens. In this study, Precirol ATO 5 and squalene were chosen as the solid and liquid cores, respectively. A variety of different emulsifiers have been used to prepare SLN and NLC, including Pluronic F68 (PF68), Myverol 18-04 K, Tween 80, and phospholipids. In addition to the skin permeation of psoralens, especially 8-MOP, the physicochemical characteristics of the obtained SLN and NLC, such as the drug loading capacity, size, zeta potential, polarity, and differential scanning calorimetry (DSC) results, were investigated. Moreover, hyperproliferative skin was used as a skin barrier for psoralen permeation in order to mimic the clinical situation.

2. Materials and methods

2.1. Materials

8-MOP, 5-MOP, TMP, squalene, and Pluronic F68 (PF68) were obtained from Sigma Chemical (St. Louis, MO, USA). Precirol ATO 5 was purchased from Gattefossé (Gennevilliers, France). Myverol 18-04 K was obtained from Quest (Naarden, The Netherlands). Tween 80 was supplied by Kanto Chemical (Tokyo, Japan). Hydrogenated soybean phosphatidylcholine (SPC, Phospholipon 80H) was from American Lecithin Company (Oxford, CT, USA).

2.2. Preparation of SLN, NLC and lipid emulsion

The oil and aqueous phases were prepared separately. The oil phase consisted of oils (12% w/v Precirol and/or squalene), lipophilic emulsifiers (0.2% w/v Myverol or SPC), and drugs (to reach a concentration of 4.4 mM in the final product), while the aqueous phase consisted of double-distilled water and hydrophilic emulsifiers (2.4% w/v PF68 or Tween 80). The two phases were heated separately to 85 °C for 15 min. The aqueous phase was added to the oil phase and mixed using a high-shear homogenizer (Pro 250, Pro Scientific, Monroe, CT, USA) for 5 min. The mixture was further treated using a probe-type sonicator (VCX600, Sonics and Materials, Newtown, CT, USA) for 10 min at 35 °C. The total volume of the final product was 10 ml. The composition of these nanoparticulate systems is demonstrated in Table 1.

2.3. Determination of particle size and zeta potential

The mean particle size (z-average) and zeta potential of the SLN and NLC were measured by photon correlation spectroscopy (Nano ZS90, Malvern, Worcestershire, UK) using a helium–neon laser with a wavelength of 633 nm. Photon correlations of spectroscopic measurements were carried out at a scattering angle of 90°. A 1:100 dilution of the formulations was made using double-distilled water before the measurement.

2.4. Determination of viscosity

The viscosity of the SLN and NLC was measured as a function of the shear rate (1/s) using a Carri-Med CSL² 100 rheometer (TA Instruments, New Castle, DE, USA). The diameters of both the cone and plate spindle were 60 mm. The determination mode was set to flow-step measurement with shear rates from 0 to 1000 1/s. The cone angle used for the measurements was 2°.

2.5. The molecular environment of SLN and NLC

The lipophilic fluorescent marker, Nile red, was used as the model solute, and the molecular environment (polarity) was elucidated by fluorometric spectroscopy based on the solvatochromism of Nile red. Emission fluorescence spectra were determined with a Hitachi F-2500 fluorescence spectrophotometer (Tokyo, Japan). The spectra of the drug carrier systems with Nile red were recorded at room temperature with both slit widths set to 10 nm. The excitation wavelength was fixed at 546 nm, and the emission spectra were recorded from 550 to 700 nm at a scanning speed of 300 nm/min.

2.6. Characterization by differential scanning calorimetry (DSC)

The broad water peak (~100 °C) in DSC may largely influence the judgement of the thermograms of the lipid nanoparticles. To avoid this interference, the SLN and NLC were freeze-dried before the DSC measurements [10,11]. DSC analysis was performed using a Q10 DSC calorimeter (TA Instruments). Powdered nanoparticles (2.5–3.5 mg) were put into aluminum pans. The thermal analysis profiles were obtained as the temperature was increased from 30 to 250 °C at a rate of 10 °C/min under nitrogen. The determination was repeated three times for the formulations from three different batches.

2.7. High-performance liquid chromatographic (HPLC) analysis of psoralens

The HPLC system included a Hitachi L-7110 pump, a Hitachi L-7200 sample processor, and a Hitachi L-7485 fluorescence

Table 1
The characterization of the formulations by particle size and zeta potential

Formulation	Lipid phase	Emulsifiers	Size (nm)	Zeta potential (mV)
SLN ^a	Precirol (12%),	PF68 ^d (2.4%) + Myverol (0.2%)	296.6 ± 49.5	−40.0 ± 5.9
NLC-PF ^b	Precirol (6%) + squalene (6%)	PF68 (2.4%) + Myverol (0.2%)	210.2 ± 14.3 [*]	−46.0 ± 2.2
NLC-Tw ^c	Precirol (6%) + squalene (6%)	T80 ^e (2.4%) + SPC ^f (0.2%)	172.7 ± 1.2 [*]	−42.3 ± 2.0
Lipid emulsion	Squalene (12%)	SPC (6%)	137.1 ± 28.5 ^{**}	−60.4 ± 8.3 ^{**}

Each value represents the mean ± SD (*n* = 3).

^a SLN, the formulation of solid lipid nanoparticles.

^b NLC-PF, the formulation of nanostructured lipid carriers with Pluronic F68 as the main emulsifier.

^c NLC-Tw, the formulation of nanostructured lipid carriers with Tween 80 as the main emulsifier.

^d PF68, Pluronic F68.

^e T80, Tween 80.

^f SPC, Soybean phosphatidylcholine.

^{*} The value is significantly lower (*p* < 0.05) as compared to the value of SLN.

^{**} The value is significantly higher (*p* < 0.05) as compared to the value of SLN.

detector. A 25-cm-long, 4-mm inner diameter stainless steel RP-18 column (Merck, Darmstadt, Germany) was used. The mobile phase consisted of methanol: double-distilled water (60:40) at a flow rate of 1 ml/min. The fluorescence detector was set to an excitation wavelength of 314 nm and an emission wavelength of 490 nm.

2.8. Capacity factor ($\log K'$)

The K' values of the psoralens were determined isocratically using HPLC. The retention time of each drug was measured and K' values were calculated from the following equation:

$$\log K' = \log (t_r - t_0) / t_0;$$

where t_r is the retention time of each drug and t_0 is the retention time of the non-retained solvent peak (methanol).

2.9. Determination of psoralen solubility in water

An excess amount of psoralens was added to 1 ml of double-distilled water and shaken reciprocally at 37 °C for 24 h. The suspension was centrifuged at 10,000 rpm for 10 min, and the drug concentration in the supernatant was determined by HPLC.

2.10. In vitro skin permeation of psoralens

The skin permeation of the psoralens was measured using a Franz diffusion assembly. The dorsal skin of female nude mice (6–8 weeks old) in a full-thickness type was mounted between the donor and acceptor compartments. The cellulose membrane (Cellu-Sep® T2, with a molecular weight cutoff of 6000–8000) was also used as a barrier in the experiments for examining psoralen release from the formulations (as shown in Fig. 7). The donor medium consisted of 0.5 ml of vehicle containing psoralens. The receptor medium (5.5 ml) was ethanol:pH 7.4 buffer (3:7) to maintain sink conditions. The available diffusion area between cells was 0.785 cm². The stirring rate and temperature were, respectively, kept at 600 rpm and 37 °C. At appropriate intervals (2, 4, 6, 8, 10, 12, and 24 h), 300-μl aliquots of the acceptor medium were withdrawn and immediately replaced with equal volumes of fresh buffer. The permeated amount of psoralens was determined by HPLC.

2.11. Induction of hyperproliferative skin for in vitro skin permeation

Epidermal hyperproliferation simulating psoriasis-affected skin was achieved by a tape-stripping technique [12]. Female nude mice (6–8 weeks old) were used in this study. The animal experiment was reviewed and approved by the Institutional Animal Care Committee at Chang Gung University. The dorsal skin of a mouse was stripped using cellophane tape (3M Scotch®) twice daily for 5 days. The stripping was repeated 10 times for each process. After 5 days, the skin was monitored by examining the transepidermal water loss (TEWL) with an evaporimeter (TM300, Courage and Khazaka, Köln, Germany). The skin was excised until the TEWL values reached 8–10 g/m²/h.

Hyperproliferation of the skin was verified by histology. Each specimen was dehydrated using ethanol, embedded in paraffin wax, and stained with hematoxylin and eosin. For each skin sample, three different sites were examined and evaluated under light microscopy (Eclipse 4000, Nikon, Tokyo, Japan). The digital photomicrographs were then processed with Adobe PhotoDeluxe (Adobe Systems, San Jose, CA, USA), and the epidermal thickness was calculated using ImagePro-plus 4.0 (Media Cybernetics, Silver Spring, MD, USA).

2.12. Statistical analysis

Statistical analysis of differences between different treatments was performed using unpaired Student's *t*-test. A 0.05 level of probability was taken as the level of significance. An analysis of variance (ANOVA) test was also used.

3. Results

3.1. Particle size and zeta potential of the SLN and NLC

The SLN and NLC were developed by hot homogenization followed by ultrasonication. Precirol, a glyceryl palmito-stearate, was used as a core material for the SLN. In the NLC formulations, squalene as the liquid matrix was mixed with Precirol into which the drug was incorporated. Squalene is an all-trans isoprenoid containing six isoprene units, which is a naturally occurring substance found in human skin. The particulate systems were stabilized with the surfactants PF68 (with a hydrophile–lipophile balance (HLB) of 29) and Myverol (with an HLB of 7). The composition of the nanoparticle shell significantly affects the physicochemical properties and drug release profiles [13]. Hence another surfactant system composed of Tween 80 (HLB of 15) and SPC (HLB of 3) was used for the NLC for comparison.

Particle sizes and surface charges of the developed SLN and NLC are shown in Table 1. It can be seen that the sizes of the SLN were significantly larger ($p < 0.05$) than those of the NLC. The particle sizes of the NLC with Tween 80 as the main emulsifier (NLC-Tw) were smaller ($p < 0.05$) than those with PF68 (NLC-PF). In order to elucidate the influence of the solid and liquid matrices on the performance of the particulate systems, a lipid emulsion with squalene (12% w/v) and SPC (6% w/v), respectively as the lipid core and emulsifier was prepared for comparison. As shown in Table 1, the lipid emulsion exhibited the smallest size ($p < 0.05$) among the formulations tested.

As depicted in Table 1, the zeta potentials of the SLN and NLC were –40 to –46 mV. No effect of the lipid core or shell on the surface charge was observed ($p > 0.05$). The lipid emulsion showed a zeta potential of –60 mV, which was significantly higher ($p < 0.05$) than those of the SLN and NLC.

3.2. Viscosity of the SLN and NLC

To develop such controlled-release formulations, rheology or viscosity is a critical parameter to consider. Furthermore, the viscous and elastic properties of the dispersions are important for their application to skin [3]. Fig. 1 shows variations in viscosity with the shear rate for the nanoparticulate systems. The appearance of the curves confirms the Newtonian behavior of the investigated formulations except for NLC-Tw. A fluctuation of viscosity between 50 and 130 1/s was observed for NLC-Tw. The viscosity varied between 0.02 and 0.05 Pa s according to the type of formulation. The SLN showed the highest viscosity, followed by the NLC and lipid emulsion. This trend was similar to the previous investigation [14], which showed a higher viscosity of SLN than NLC.

3.3. Molecular environment of the SLN and NLC

Nile red is a dye whose absorption bands vary in shape, position, and intensity with the nature of the environment. The emission spectra of Nile red in the nanoparticulate systems are shown in Fig. 2. Nile red is very soluble in organic solvents such as acetone and strongly fluorescent in a lipophilic environment [15]. Corresponding to high lipophilicity such as with acetone and squalene, the emission maximum was found to be near 600 nm.

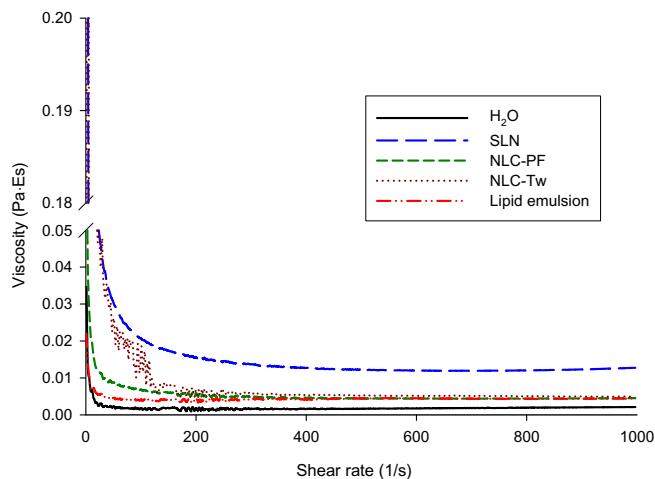


Fig. 1. Viscosity (Pa s) versus the shear rate (1/s) of the nanoparticulate systems.

When incorporated into the SLN, the increased re-orientation probability of the surrounding water molecules led to emission shifts to longer wavelengths. NLC-PF and the lipid emulsion exhibited a wavelength shift as well as a reduction in the fluorescence intensity. This is because the fluorescence is quenched in a more hydrophilic environment [16]. The results indicate an increasing trend of hydrophilicity of the lipid emulsion > NLC-PF > NLC-Tw > SLN.

3.4. DSC characterization

DSC uses the fact that different lipid modifications possess different melting points. Fig. 3 shows DSC curves of Precirol, the physical mixture, and lyophilized nanoparticulate systems with or without 8-MOP. The lipid emulsions were not examined by DSC because liquids such as squalene cannot be registered using the described temperatures and analytical conditions. Precirol alone exhibits a peak at 58 °C with a shoulder at 62 °C as seen in Fig. 3A. Different polymorphs of complex glycerides often show several diffuse melting maxima or peak shoulders in DSC [17]. 8-MOP

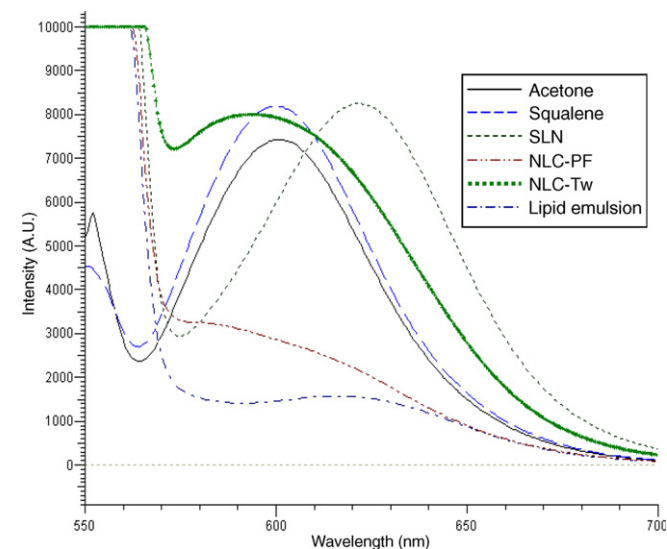


Fig. 2. Fluorescence emission spectra of Nile red ($2.5 \times 10^{-5}\%$, w/v) in acetone, squalene, and nanoparticulate systems. SLN, solid lipid nanoparticles; NLC-PF, nanostructure lipid carriers with PF68 as a hydrophilic emulsifier; NLC-Tw, nanostructure lipid carriers with Tween 80 as a hydrophilic emulsifier. A.U. in the x-axis means arbitrary unit.

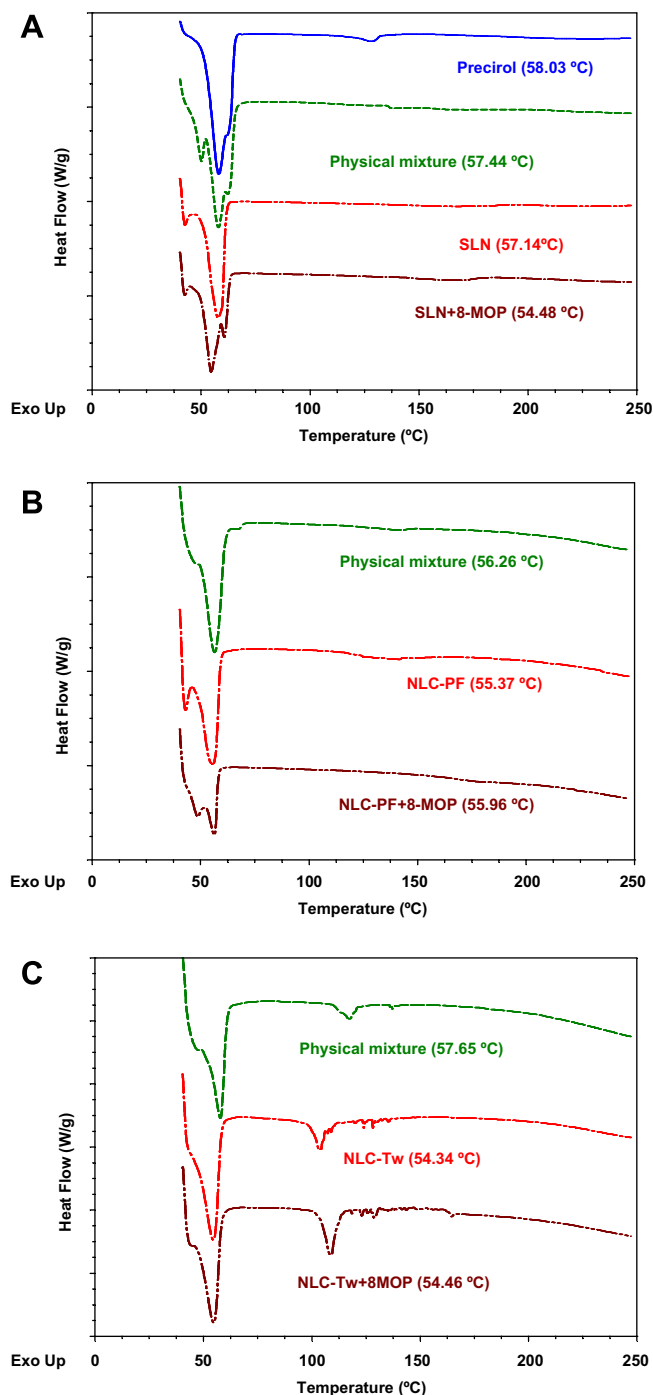


Fig. 3. Heating curves of differential scanning calorimetry (DSC) for Precirol, the physical mixture, and nanoparticulate systems with or without 8-MOP (4.4 mM): (A) solid lipid nanoparticles (SLN); (B) nanostructured lipid carrier + PF68 (NLC-PF); and (C) NLC + Tween (NLC-Tw).

showed a melting point at 142 °C. The DSC measurements revealed no drug peak for any of the particles around 142 °C (Fig. 3A). The peak of Precirol in the SLN loaded with 8-MOP showed a shift from 58 to 54 °C. Some peaks observed around 45 °C in Fig. 3 were endothermic start-up hooks, which were produced in the initial equilibrium process because of the slightly different temperatures between sample pan and reference pan.

A depression of Precirol's melting point (58 to 56 °C) was detected in the NLC-PF physical mixture (Fig. 3B). This phenomenon was not observed for the SLN. This indicates an interaction of liquid squalene with the crystalline Precirol matrix. The melting point

was further reduced from 58 to 55 °C for the lyophilized NLC-PF system. There was no depression of the melting point for the NLC-Tw physical mixture (Fig. 3C). The endothermic peak at 115 °C is the flash point of Tween 80. The flash point of a liquid is the lowest temperature at which it can form an ignitable mixture in air. An interaction between squalene and Precirol occurred after preparing NLC-Tw, resulting in a depression of the melting point (58 to 54 °C). The presence of 8-MOP did not influence the thermograms of NLC-Tw.

3.5. Skin permeation of psoralens released from the SLN and NLC

In order to evaluate the skin targeting potential of the SLN and NLC, the permeation ability of psoralens through the skin was examined *in vitro*. A previous study indicated that the total 8-MOP permeation through the skin corresponds to the accumulation of 8-MOP in the skin [9]. Hence the drug flux permeated across the skin may be an indicator of the drug deposition within the skin reservoir in the case of psoralen. The cumulative amounts of 8-MOP at different times in the acceptor are shown in Fig. 4, and the steady-state fluxes (nmol/cm²/h) are summarized in Table 2. The permeation followed zero-order kinetics for the nanoparticulate systems ($r > 0.98$). For the aqueous suspension (4.4 mM 8-MOP in double-distilled water), a biphasic drug release pattern was observed. A relative burst of drug permeation was found in the initial 10 h, after which the drug slowly permeated with a linear relationship on the Higuchi plot. The drug flux was found to be the highest for both NLC vehicles ($p < 0.05$). There was no improvement in skin permeation over the aqueous control with the SLN ($p > 0.05$). The flux with the lipid emulsion was even lower ($p < 0.05$) than that of the aqueous suspension.

The derivatives of 8-MOP, 5-MOP, and TMP were also chosen as permeants in the *in vitro* permeation study. As shown in Table 2, the permeation ability increased in the order of 8-MOP > 5-MOP > TMP. The permeation trends of the various vehicles for the three drugs were similar, with NLC showing the best delivery. The TMP flux from NLC-PF was significantly higher ($p < 0.05$) than that from NLC-Tw, whereas no significant difference ($p > 0.05$) between the two vehicles was observed for 8-MOP and 5-MOP.

3.6. Skin permeation of 8-MOP across hyperproliferative skin

8-MOP and related furocoumarins are extensively used for treating hyperproliferative skin diseases. Fig. 5 depicts representa-

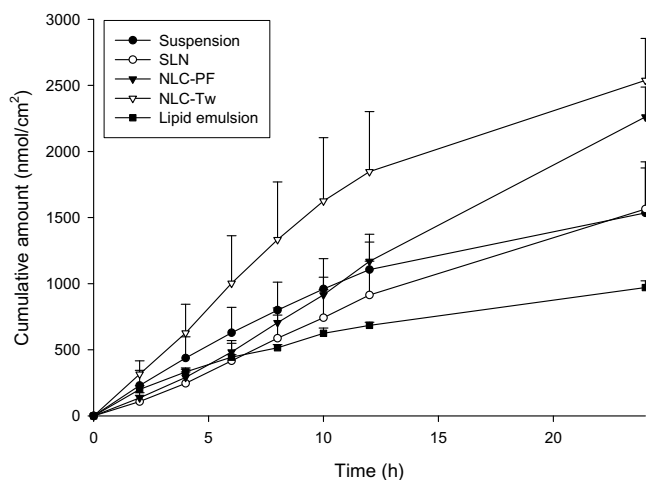


Fig. 4. In vitro cumulative amount (nmol/cm²)–time profiles of the skin permeation of 8-MOP (4.4 mM) from an aqueous suspension and nanoparticulate systems. Each value represents the mean \pm SD ($n = 4$).

Table 2

The flux (nmol/cm²/h) of psoralens across nude mouse skin

Formulation	8-MOP ^a	5-MOP ^b	TMP ^c
Suspension ^d	60.48 \pm 15.69 ^h	15.88 \pm 4.48	1.90 \pm 0.09
SLN ^e	67.17 \pm 8.89	16.06 \pm 2.14	2.70 \pm 0.41
NLC-PF ^f	96.71 \pm 6.22	20.46 \pm 3.60	4.03 \pm 0.66
NLC-Tw ^g	107.51 \pm 8.57	25.18 \pm 3.62	2.34 \pm 0.31
Lipid emulsion	38.31 \pm 5.31	8.77 \pm 0.63	1.46 \pm 0.26

Each value represents the mean \pm SD ($n = 4$).

^a 8-MOP, 8-methoxypsoralen.

^b 5-MOP, 5-methoxypsoralen.

^c TMP, 4,5,8-trimethylpsoralen.

^d Suspension, psoralens (4.6 mM) in double-distilled water.

^e SLN, the formulation of solid lipid nanoparticles.

^f NLC-PF, the formulation of nanostructured lipid carriers with Pluronic F68 as the main emulsifier.

^g NLC-Tw, the formulation of nanostructured lipid carriers with Tween 80 as the main emulsifier.

^h This flux was calculated based on zero-order equation although the Higuchi model showed a higher correlation coefficient.

tive examples of light microscopic images of vertical skin sections with or without hyperproliferative induction. As shown in Fig. 5B, the tape-stripping technique increased the epidermal thickness by 1.5-fold. The estimated thicknesses of the epidermis with and without tape-stripping were 27.9 \pm 4.4 and 18.2 \pm 4.3 μ m, respectively. Routine light microscopy confirmed the predominant changes of the psoriasis-like skin.

Fig. 6 compares 8-MOP fluxes across normal and hyperproliferative skin. The SLN and NLC-Tw showed no significant differences ($p > 0.05$) in 8-MOP permeation between the two skin types. On the other hand, hyperproliferative skin exhibited lower drug permeation compared to normal skin with the other formulations; in particular, the aqueous suspension showed the greatest difference.

4. Discussion

PUVA photochemotherapy is widely used to treat skin diseases such as psoriasis, mycosis fungoides, and vitiligo. In this study, we investigated the skin permeation of nanoparticulate systems loaded with psoralens commonly used in this therapy. This study indicates that physicochemical characteristics and drug delivery can be greatly affected by changing the materials used in the SLN and NLC. We showed that both enhanced and controlled permeation of psoralens can be achieved by the vehicles developed herein.

Nano- and submicron-sized particles can be obtained for the prepared SLN and NLC. The crystalline lipid core (of the SLN) produced a larger particle diameter compared to the amorphous core (of the NLC). Even though a negative zeta potential provides electrostatic repulsion to maintain the small size of these systems, Tween 80 also provides steric stability [1,18]. This was the reason for the smaller size of NLC-Tw compared to NLC-PF.

The lipid emulsion exhibited a higher charge than either the SLN or NLC. The origin of the negative charge of the emulsion was the anionic fractions of SPC. SPC used in this study contained 80% PC, which is uncharged. The other components (20%) of SPC are negatively charged. Profiles of the zeta potential confirm the smaller size of the lipid emulsion compared to the SLN and NLC, since greater ionization at the interface tends to increase the electrostatic repulsion and prevent aggregation [19]. Both PF68 and Tween 80 are non-ionic species. The lipophilic emulsifiers, Myverol (palmitic acid monoglycerides) and SPC, in the interface of the SLN and NLC may be responsible for the negative surface charges. Measuring the zeta potential allows predictions of the storage stability [20]. In general, particle aggregation is less likely to occur for particles with surface charges >30 mV.

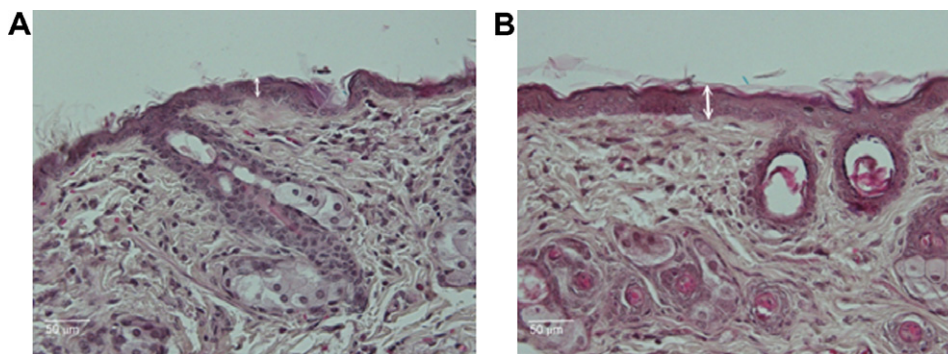


Fig. 5. Histologic examination of nude mouse back skin in (A) the non-treated control group and (B) the group subjected to a tape-stripping technique. Arrows indicate the thickness of the epidermis (magnification 400 \times). The bar length indicates 50 μ m.

The presence of Precirol in the systems resulted in increased viscosity. Thus the viscosity increased in the order of SLN > NLC > the lipid emulsion. The viscosity may be related to the strength of the interfacial film [21]. This suggests that the SLN had stronger films, which may have been due to the crystalline state of the inner lipid phase.

As demonstrated in Fig. 2, the SLN exhibited a more lipophilic environment than the other systems. The pronounced lipophilic character of Precirol expressed by a low HLB of 2 may have contributed to this result. A sufficient amount of emulsifiers is needed for the lipid core with high lipophilicity or percentage in oil-in-water systems [22]. A deficit of emulsifiers may cause a larger size of \sim 300 nm for SLN (Table 1). The lipophilicity decreased following an increase in the squalene content in the formulations. NLC-Tw is more lipophilic than NLC-PF. This may have been due to Tween 80 and SPC producing a less-hydrophilic emulsifier system compared to PF68 and Myverol according to the HLB values. This suggests that both the inner core and interfacial film affected the molecular environment of SLN and NLC.

The DSC thermograms of the lyophilized SLN and NLC did not show a melting peak for 8-MOP. This absence may have been due to solubilization of the low amount of the drug (0.1% w/v) in the molten lipid when the sample was heating up. This result was confirmed by a physical mixture loaded with 8-MOP, which also revealed the absence of a drug peak (data not shown). The thermograms showed that the endothermic peak of Precirol did not change after being incorporated into the SLN system. This sug-

gests a higher-ordered lattice arrangement in the lipid cores. However, the loading of 8-MOP in the SLN resulted in a depression of the Precirol peak. The drug present in the lipid matrix seemed to accelerate the polymorphic transition to a stable modification in comparison to drug-free particles. This result was attributed to interactions between the lipids and drug molecules and differences in the drug deposition within particles [23].

The presence of a glass transition in the DSC thermograms of the NLC points to the crystalline nature of the NLC particles, whereas the melting points in the NLC were depressed when compared with that of the corresponding bulk Precirol. Defects in the crystalline lattice may have contributed to this depression. It may also have been due to the smaller particle sizes of the NLC as compared to the SLN. The reduced particle size and increased surface area led to a decrease in the melting enthalpy compared with the heat flow through the larger crystals. This was confirmed by physical mixtures for which this type of depression was insignificant. This depression was especially meaningful for NLC-Tw. This may have been due to the more lipophilic emulsifiers used in NLC-Tw. Tween 80 and SPC in the interfacial film may interact with the lipid core to a great degree, modifying the crystalline state. Because the melting point of Precirol was depressed, the phase separation of Precirol and squalene can be excluded.

8-MOP was mainly used as the model drug for the *in vitro* skin permeation study. 5-MOP and TMP were chosen as secondary model drugs in order to elucidate the influences of chemical structure and lipophilicity. All these drugs have limited water solubilities and high lipophilicities which make them excellent candidates for SLN and NLC encapsulation (Table 3).

An inverse relation exists between drug permeation and lipophilicity ($\log K'$) of psoralens permeated from the aqueous suspension. Since 4.4 mM psoralen could not be completely solubilized in water, the low level of TMP permeation may have been due to the poor water solubility of TMP (Table 3). The permeants should pass

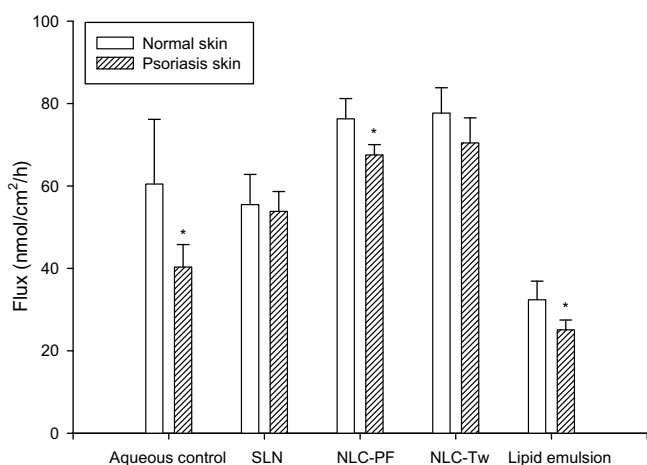


Fig. 6. Comparison of the 8-MOP fluxes from an aqueous suspension and nanoparticulate systems across normal and hyperproliferative skin. Each value represents the mean \pm SD ($n = 4$).

Table 3
The $\log K'$ and solubility profiles of psoralens

Compound	$\log K'^a$	Solubility in water (nmol/ml)	K_p (cm/h $\times 10^{-2}$) ^b
8-MOP ^c	0.30 \pm 0.002	229.20 \pm 14.49	3.58 \pm 0.06
5-MOP ^d	0.56 \pm 0.004	15.14 \pm 0.99	4.45 \pm 0.13
TMP ^e	1.12 \pm 0.002	0.46 \pm 0.10	7.50 \pm 2.20

Each value represents the mean \pm SD ($n = 5$).

^a $\log K'$, logarithm of $t_r - t_0/t_0$, t_r is the retention time of product peak, t_0 is the retention time of solvent peak.

^b K_p , permeability coefficient = flux from water with saturated drug solubility/drug solubility in water.

^c 8-MOP, 8-methoxypsoralen.

^d 5-MOP, 5-methoxypsoralen.

^e TMP, 4,5,8-trimethylpsoralen.

through the skin in a solubilized state. A further permeation experiment was performed by testing the skin permeation at a dose of saturated solubility in the donor compartment. A saturated drug solution was used to ensure uniform thermodynamic activities. The permeability coefficient (K_p , cm/h) was calculated from the flux divided by the dose applied to the donor compartment (Table 3). It was observed that the K_p values were related to the lipophilicity of psoralens. The trend of K_p of various psoralens was quite different from that of the flux from aqueous suspension in a regular dose (4.4 mM). The result indicates that the solubility in water dominated psoralen permeation from the aqueous suspension.

Compared to the lipid emulsion and aqueous control, enhanced psoralen permeation and controlled release were achieved with the SLN and NLC. For dermal applications, both features are of interest. Enhanced permeation can be useful to improve drug penetration. Sustained release becomes important to supply the skin with a drug over a prolonged period of time [17]. The release from the internal phase supplements depletion of the drug in the external phase, supplying sustained and controlled release of the drug into the skin [24,25]. Factors contributing to the increased skin delivery by SLN and NLC include solubility enhancement, the large surface area due to small particle sizes, an occlusive effect, and a permeation enhancer effect [3,26]. The simplest mechanism for enhancing permeation is that psoralens can readily be dissolved in SLN and NLC but not in water. Hence the higher drug loading in the systems increased the concentration gradient towards the skin. However, TMP still showed a poorer delivery from the SLN and NLC compared to the other formulations. The drug should be released from the internal to the external phase and then from the external phase to the skin. The extremely low water solubility may have caused the difficulty of TMP diffusion from the lipid core to the aqueous phase.

The bioavailability of drugs penetrating the skin can be enhanced by using nanoparticulate systems because the small particle size ensures close contact with the SC. Small droplets have better chances to adhere to the skin and transport the drugs in a more controlled fashion [24]. It is difficult for nanoparticles transport into the skin in an intact form because of the limited voids in the lipid bilayers of SC. It is assumed that the SLN and NLC form films of densely packed spheres on the surface of the skin, which exert an occlusive effect, thus increasing skin hydration [20,26]. Due to the smaller particle size, NLC may have a more favorable occlusive effect than SLN. Another possible reason for the high drug permeation of NLC is the reduced viscosity. In most cases, the lower the viscosity of the vehicle, the faster is the drug delivery [24,27]. Although the size reduction, occlusive effect, and viscosity may explain the greater permeation of NLC than SLN, they are not general rules in this since the lipid emulsion had the lowest particle diameter and viscosity. The permeation of psoralens into skin might not solely be controlled by these factors.

The lipid emulsion possessed a high zeta potential of -60 mV. The surface of the skin carries negative charges due to the presence of negatively charged residues of proteins. It is anticipated that a delivery system with a highly negative charge that is strongly excluded by the skin would result in poor permeation [28,29]. Another reason is that non-crystalline lipid nanoparticles have no occlusive properties [30].

The enhanced skin permeation of the nanoparticulate vehicles was probably due to the additives included in the formulation. Surfactants, which can loosen or fluidize the lipid bilayers of the SC, can act as permeation enhancers. To investigate the enhancing potential of the surfactants, the skin was pretreated with solutions of surfactants at the same concentration as in the systems for 2 h, followed by administering 8-MOP in an aqueous suspension for in vitro permeation. The pretreatment method avoids a cosolvent ef-

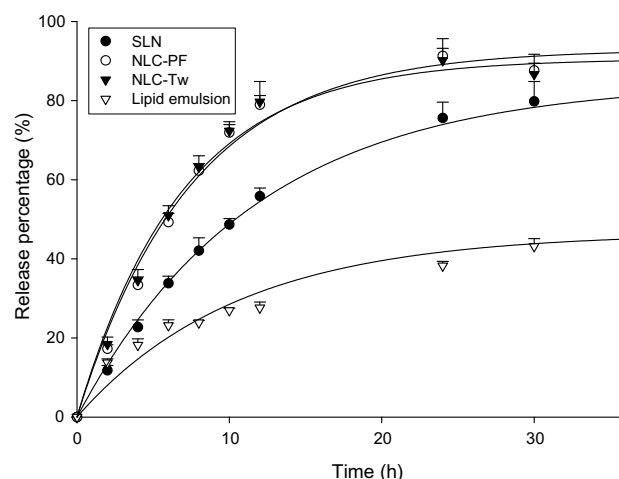


Fig. 7. In vitro release percentage (%)–time profiles of 8-MOP (4.4 mM) from an aqueous suspension and nanoparticulate systems across a cellulose membrane. Each value represents the mean \pm SD ($n = 4$).

fect on the thermodynamic activities of the drugs and enhancers. The results showed that no surfactant produced any enhancement of 8-MOP permeation compared to pretreatment with water ($p > 0.05$, data not shown). Hence the enhancer effect could be ignored.

The NLC provided higher drug fluxes than the SLN. The incorporation of liquid lipids into the solid lipid matrix caused the NLC to become more imperfect as demonstrated by DSC. Thus the loaded drug was more easily released, increasing the drug release rate. On the other hand, drug molecules are incorporated into the crystalline matrix, and their diffusion mobility is decreased [31,32]. In order to elucidate the mechanism, the ability of the SLN and NLC to deliver 8-MOP was investigated by determining the release rates across a cellulose membrane. In the process of skin permeation, the drug should firstly release from the vehicles, then it can be partitioned into or absorbed by the skin. As shown in Fig. 7, the release of 8-MOP showed an initial burst that gradually leveled off after 12 h of administration. 8-MOP was released to a greater extent from both NLC vehicles. Although diffusion mobility may be the possible mechanism for the release profile, it still cannot explain the relatively low release rate of the lipid emulsion. Since the zeta potential might not affect drug release across the cellulose membrane, the lack of an occlusive ability for the emulsion is a possible cause of this low release. The trends of release rates from various systems were the same as those of the fluxes, suggesting that the process of 8-MOP permeation into the skin is vehicle-controlled but not skin-controlled.

It was found that variations in the types of emulsifiers in the NLC had no profound effects on 8-MOP fluxes or release rates ($p > 0.05$). However, NLC-PF provided higher TMP permeation than did NLC-Tw. The lipophilic interfacial films produced by Tween 80 and SPC may have strongly interacted with TMP, which showed the most lipophilic nature among psoralens, resulting in difficulty of TMP being released from the inner phase.

Psoriasis is a disorder triggered when activated immunocytes infiltrate the skin, subsequently inducing prominent epidermal thickening. Two methods can induce psoriasis skin in animal models: xenografts in mice and tape-stripping techniques [12,33]. We used the latter method to create hyperproliferative skin. It was confirmed that the tape-stripping method can induce psoriasis-like skin characterized by epidermal hyperplasia. A similar result was observed in the study by Denda et al. [34]. Some vehicles showed a slight but significant reduction in 8-MOP permeation in hyperproliferative skin, including NLC-PF and the lipid emulsion.

A greater reduction in drug permeation across psoriasis-like skin was observed for the aqueous control. This reduction may have been due to the increment in thickness of the epidermis, creating a longer pathway through which the drug had to pass. The result indicates that the use of nano-sized particles can minimize 8-MOP permeation differentiation between normal and disordered skin. This may be especially important for patients with severe psoriasis who have a relatively thick epidermis. Most research papers have utilized healthy skin to examine drug permeation, and results from such studies might not be appropriately applied to predict the skin targeting ability of a drug on disordered skin. The skin model used in this study may be useful for resolving this problem.

5. Conclusions

Psoriasis often reoccurs and is rarely cured, and hence patients may receive therapy periodically over many years. Hence developing efficient vehicles for delivering psoralens to treat psoriasis is especially important. SLN and NLC formulations were developed in this study to achieve this aim. Nano- to submicron-sized particles can be achieved with SLN and NLC, and the NLC showed smaller-sized particles. Enhanced permeation and controlled release of psoralens were obtained with NLC. Enhanced permeation can be useful for improving the skin absorption of drugs, while sustained release is important for drugs with irritating effects at high concentrations or to supply the skin with drugs over a prolonged period of time. According to the *in vitro* study, psoralen permeation can be controlled by altering the formulation variables. Solubility enhancement, small particle sizes, and an occlusive effect of NLC may be possible mechanisms for the enhancement. The results indicated that the NLC prepared in this study can potentially be exploited as carriers with improved drug permeation for psoriasis therapies.

References

- [1] J. Liu, W. Hu, H. Chen, Q. Ni, H. Xu, X. Yang, Isotretinoin-loaded solid lipid nanoparticles with skin targeting for topical delivery, *Int. J. Pharm.* 328 (2007) 191–195.
- [2] Z. Mei, H. Chen, T. Wang, Y. Yang, X. Yang, Solid lipid nanoparticle and microemulsion for topical delivery of triptolide, *Eur. J. Pharm. Biopharm.* 56 (2003) 189–196.
- [3] R.H. Müller, M. Radtke, S.A. Wissing, Solid lipid nanoparticles (SLN) and nanostructured lipid carriers (NLC) in cosmetic and dermatological preparations, *Adv. Drug Deliv. Rev.* 54 (2002) S131–S155.
- [4] M.A. Lowes, A.M. Bowcock, J.G. Krueger, Pathogenesis and therapy of psoriasis, *Nature* 445 (2007) 866–873.
- [5] S.N. Al-Suwaidan, S.R. Feldman, Clearance is not a realistic expectation of psoriasis treatment, *J. Am. Acad. Dermatol.* 42 (2000) 796–802.
- [6] F.P. Gasparro, The role of PUVA in the treatment of psoriasis, *Am. J. Clin. Dermatol.* 1 (2000) 337–348.
- [7] D. Bethea, B. Fullmer, S. Syed, G. Seltzer, J. Tiano, C. Rischko, L. Gillespie, D. Brown, F.P. Gasparro, Psoralen photobiology and photochemotherapy: 50 years of science and medicine, *J. Dermatol. Sci.* 19 (1999) 78–88.
- [8] M. Grundmann-Kollmann, S. Behrens, R.U. Peter, M. Kerscher, Treatment of severe and recalcitrant dermatoses of the palms and soles with PUVA-bath versus PUVA-cream therapy, *Photodermatol. Photoimmunol. Photomed.* 15 (1999) 87–89.
- [9] B. Baroli, M.A. López-Quintela, M.B. Delgado-Charro, A.M. Fadda, J. Blanco-Méndez, Microemulsions for topical delivery of 8-methoxsalen, *J. Control. Release* 69 (2000) 209–218.
- [10] R. Cavalli, O. Caputo, M.R. Gasco, Preparation and characterization of solid lipid nanospheres containing paclitaxel, *Eur. J. Pharm. Sci.* 10 (2000) 305–309.
- [11] E. Vighi, B. Ruozzi, M. Montanari, R. Battini, E. Leo, Re-dispersible cationic solid lipid nanoparticles (SLNs) freeze-dried without cryoprotectors: characterization and ability to bind pEGFP-plasmid, *Eur. J. Pharm. Biopharm.* 67 (2007) 320–328.
- [12] M. Demerjian, M.Q. Mao, E.H. Choi, B.E. Brown, D. Crumrine, S. Chang, T. Mauro, P.M. Elias, K.R. Feingold, Topical treatment with thiazolidinediones, activators of peroxisome proliferators-activated receptor- γ , normalizes epidermal homeostasis in a murine hyperproliferative disease model, *Exp. Dermatol.* 15 (2006) 154–160.
- [13] B.D. Kim, K. Na, H.K. Choi, Preparation and characterization of solid lipid nanoparticles (SLN) made of cacao butter and curdlan, *Eur. J. Pharm. Sci.* 24 (2005) 199–205.
- [14] A. Saupé, S.A. Wissing, A. Lenk, C. Schmidt, R.H. Müller, Solid lipid nanoparticles (SLN) and nanostructured lipid carriers (NLC) – structural investigations on two different carrier systems, *Bio-Med. Mater. Eng.* 15 (2005) 393–402.
- [15] S. Lombardi Borgia, M. Regehy, R. Sivaramakrishnan, W. Mehnert, H.C. Korting, K. Danker, B. Röder, K.D. Kramer, M. Schäfer-Korting, Lipid nanoparticles for skin penetration enhancement – correlation to drug localization within the particle matrix as determined by fluorescence and parelectric spectroscopy, *J. Control. Release* 110 (2005) 151–163.
- [16] K. Jores, A. Haberland, S. Wartewig, K. Mäder, W. Mehnert, Solid lipid nanoparticles (SLN) and oil-loaded SLN studied by spectrofluorometry and Raman spectroscopy, *Pharm. Res.* 22 (2005) 1887–1897.
- [17] V. Jenning, M. Schäfer-Korting, S. Gohla, Vitamin A-loaded solid lipid nanoparticles for topical use: drug release properties, *J. Control. Release* 66 (2000) 115–126.
- [18] W. Weyenberg, P. Filev, D. Van den Plas, J. Vandervoort, K. DeSmet, P. Sollié, A. Ludwig, Cytotoxicity of submicron emulsions and solid lipid nanoparticles for dermal application, *Int. J. Pharm.* 337 (2007) 291–298.
- [19] D.F. Driscoll, Lipid injectable emulsions: pharmacopeial and safety issues, *Pharm. Res.* 23 (2006) 1959–1969.
- [20] R.H. Müller, K. Mäder, S. Gohla, Solid lipid nanoparticles (SLN) for controlled drug delivery – a review of the state of the art, *Eur. J. Pharm. Biopharm.* 50 (2000) 161–177.
- [21] T.G. Mason, New fundamental concepts in emulsion rheology, *Curr. Opin. Colloid Interf. Sci.* 4 (1999) 231–238.
- [22] C.F. Hung, J.K. Chen, M.H. Liao, H.M. Lo, J.Y. Fang, Development and evaluation of emulsion-liposome blends for resveratrol delivery, *J. Nanosci. Nanotechnol.* 6 (2006) 2950–2958.
- [23] A. zur Mühlen, C. Schwarz, W. Mehnert, Solid lipid nanoparticles (SLN) for controlled drug delivery – drug release and release mechanism, *Eur. J. Pharm. Biopharm.* 45 (1998) 149–155.
- [24] A. Kogan, N. Garti, Microemulsions as transdermal drug delivery vehicles, *Adv. Colloid Interf. Sci.* 123–126 (2006) 369–385.
- [25] J.J. Wang, K.C. Sung, O.Y.P. Hu, C.H. Yeh, J.Y. Fang, Submicron lipid emulsion as a drug delivery system for nalbuphine and its prodrugs, *J. Control. Release* 115 (2006) 140–149.
- [26] H. Chen, X. Chang, D. Du, W. Liu, J. Liu, T. Weng, Y. Yang, H. Xu, X. Yang, Podophyllotoxin-loaded solid lipid nanoparticles for epidermal targeting, *J. Control. Release* 110 (2006) 296–306.
- [27] M. Trotta, E. Ugazio, E. Peira, C. Pulitano, Influence of ion pairing on topical delivery of retinoic acid from microemulsions, *J. Control. Release* 86 (2003) 315–321.
- [28] M.P. Youenang Piemi, D. Kornev, S. Benita, J. Marty, Positively and negatively charged submicron emulsions for enhanced topical delivery of antifungal drugs, *J. Control. Release* 58 (1999) 177–187.
- [29] J.Y. Fang, Y.L. Leu, C.C. Chang, C.H. Lin, Y.H. Tsai, Lipid nano/submicron emulsions as vehicles for topical flurbiprofen delivery, *Drug Deliv.* 11 (2004) 97–105.
- [30] S.A. Wissing, R.H. Müller, The influence of the crystallinity of lipid nanoparticles on their occlusive properties, *Int. J. Pharm.* 242 (2002) 377–379.
- [31] K. Westesen, H. Bunjes, M.H.J. Koch, Physicochemical characterization of lipid nanoparticles and evaluation of their drug loading capacity and sustained release potential, *J. Control. Release* 48 (1997) 223–236.
- [32] F.Q. Hu, S.P. Jiang, Y.Z. Du, H. Yuan, Y.Q. Ye, S. Zeng, Preparation and characteristics of monostearin nanostructured lipid carriers, *Int. J. Pharm.* 314 (2006) 83–89.
- [33] B.J. Nickoloff, B. Bonish, B.B. Huang, S.A. Porcelli, Characterization of a T cell line bearing natural killer receptors and capable of creating psoriasis in a SCID mouse model system, *J. Dermatol. Sci.* 24 (2000) 212–225.
- [34] M. Denda, L.C. Wood, S. Emami, C. Calhoun, B.E. Brown, P.M. Elias, K.R. Feingold, The epidermal hyperplasia associated with repeated barrier disruption by acetone treatment or tape stripping cannot be attributed to increased water loss, *Arch. Dermatol. Res.* 288 (1996) 230–238.